iScience

CellPress
OPEN ACCESS

Article

The mechanisms and therapeutic potential of clopidogrel in mitigating diabetic cardiomyopathy in db/db mice

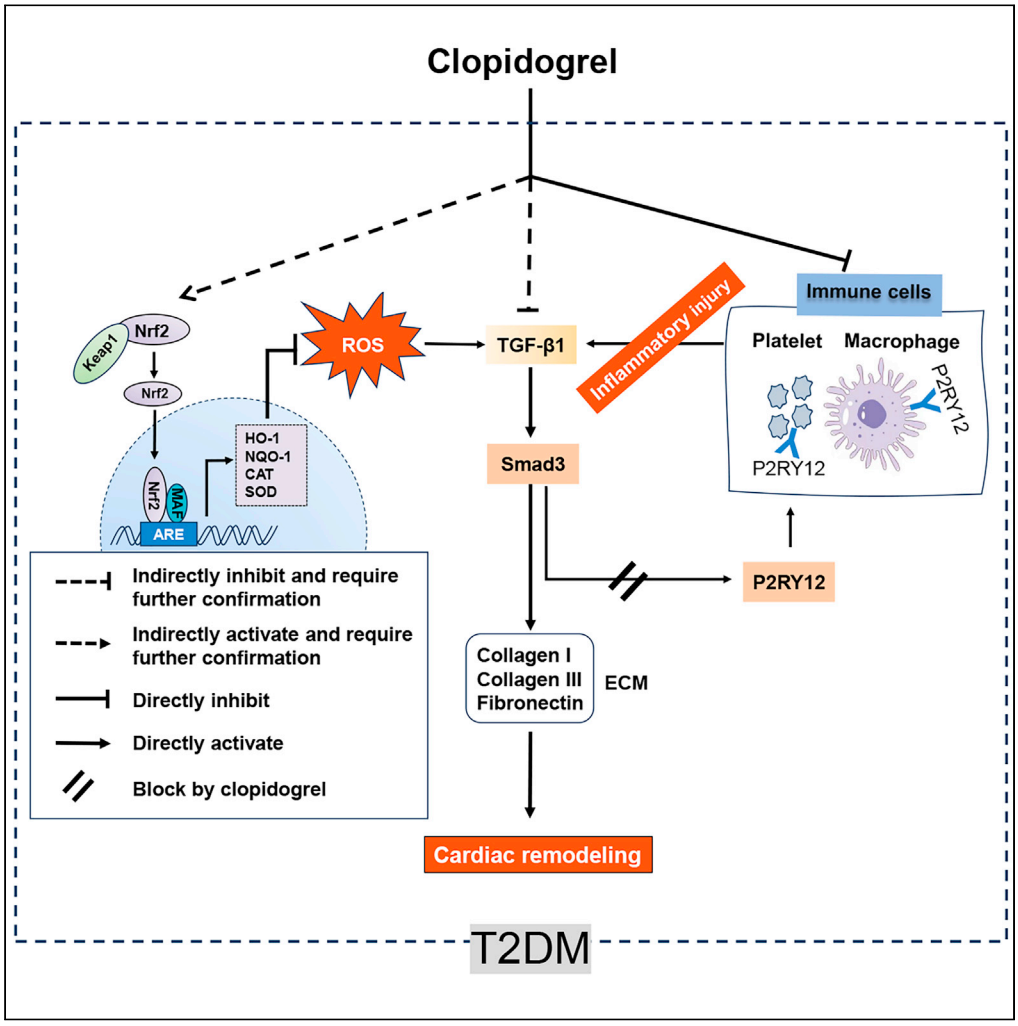

Bing Li, Yaoting Zhang, Yang Zheng, He Cai

zhengyang@jlu.edu.cn (Y.Z.)
caihe19@mails.jlu.edu.cn (H.C.)

Highlights

Clopidogrel alleviates diabetes-induced cardiac hypertrophy and dysfunction in mice

Clopidogrel treatment effectively blocks TGF-β1/Smad3/P2RY12 pathway in db/db mice

P2RY12 might be an effective target for the treatment of diabetic cardiomyopathy

Clopidogrel protects against cardiac oxidative damage by induction of Nrf2 pathway

Li et al., iScience 27, 109134
March 15, 2024
https://doi.org/10.1016/j.isci.2024.109134

iScience

CellPress
OPEN ACCESS

Article

The mechanisms and therapeutic potential of clopidogrel in mitigating diabetic cardiomyopathy in db/db mice

Bing Li,[1] Yaoting Zhang,[1] Yang Zheng,[1,*] and He Cai[1,2,*]

SUMMARY

Clopidogrel has been shown to play a protective role against diabetic nephropathy. However, whether clopidogrel exerts a protective effect against diabetic cardiomyopathy (DCM) is unknown. Three-month-old male db/db mice were administered clopidogrel daily at doses of 5, 10, and 20 mg/kg by gavage for 5 months. Here, we showed that clopidogrel effectively attenuated diabetes-induced cardiac hypertrophy and cardiac dysfunction by inhibiting cardiac fibrosis, inflammatory responses, and oxidative stress damage in db/db mice. Diabetes-induced cardiac fibrosis was inhibited by clopidogrel treatment via blockade of the TGF-β1/Smad3/P2RY12 pathway and inhibition of macrophage infiltration in db/db mice. The protective effects of clopidogrel against oxidative damage were mediated by the induction of the Nrf2 signaling pathway. Taken together, our findings provide strong evidence that clopidogrel is a promising effective agent for the treatment of DCM by alleviating diabetes-induced cardiac hypertrophy and dysfunction. P2RY12 might be an effective target for the treatment of DCM.

INTRODUCTION

Diabetes mellitus (DM) carries a substantial global burden, and at least 640 million people are expected to develop type-2 diabetes mellitus (T2DM) by 2040.[1] T2DM is a chronic disease, and over time hyperglycaemia and hyperlipidemia induced by diabetes lead to irreversible damage to multiple organs.[2] In particular, patients with diabetes are more likely to develop cardiovascular disease,[3] and diabetic cardiomyopathy (DCM) has a poor prognosis.[4] The disease was initially identified in patients with diabetes who exhibited cardiac dysfunction and structural abnormalities in the absence of coronary artery disease, hypertension, or heart valve disease.[2,5,6] DCM is usually characterized by diffuse myocardial fibrosis, cardiac hypertrophy, excessive reactive oxygen species (ROS) production, and inflammatory responses, which ultimately lead to cardiac dysfunction.[7–9]

Extensive evidence has shown that inflammatory responses, ROS accumulation, and cardiac fibrosis are hallmark mediators of DCM development.[2,7,9,10] Elevated oxidative stress-induced damage and inflammation induced by hyperglycaemia further accelerate cardiac fibrosis and cardiac dysfunction.[11,12] Extracellular matrix (ECM) generation is a key marker of myocardial fibrosis. The components of the ECM mainly include collagen, elastin, fibronectin, and laminin. In particular, collagen deposition (especially that of type-I and type-III collagens) is a vital feature of cardiac fibrosis.[13] ECM deposition leads to increased cardiac stiffness and decreased ventricular compliance, impairing the normal diastolic and systolic functions of the heart and eventually contributing to heart failure.

Thus, agents with anti-inflammatory, antioxidant, and antifibrotic effects are expected to be effective in DCM treatment. The purinergic receptor P2Y12 (P2RY12), which is expressed primarily on the surface of platelets, is also expressed by macrophages with a macrophage-to-myofibroblast transition phenotype.[14] Clopidogrel (Clo), an oral antiplatelet drug that irreversibly binds to P2RY12, has been revealed to have numerous biological impacts, such as anti-inflammatory, antioxidative, and antifibrotic effects.[14–17] Extensive evidence indicates that Clo prevents the release of inflammatory markers that promote myocardial remodeling.[17,18] Moreover, P2RY12 gene knockout in mice alleviates cardiac remodeling and improves cardiac function by inhibiting cardiac fibrosis, inflammatory responses, and macrophage infiltration in mice with pressure overload-induced hypertrophy.[17] In addition, Clo was recently shown to alleviate renal fibrosis by preventing macrophage-to-myofibroblast transition and inhibiting transforming growth factor β (TGF-β).[14] Furthermore, Clo can exert antioxidant effects by activating the nuclear factor erythroid 2-related factor 2 (Nrf2) pathway.[16] Other studies reported that Clo treatment reversed diabetic nephropathy by inhibiting fibrosis and inflammation.[19,20]

To date, the possible protective effect of Clo against DCM has not been investigated, which prompted this study. Therefore, our study explored whether Clo exerts a protective effect on DCM in db/db mice and the underlying mechanisms involved.

[1]Department of Cardiovascular Diseases, The First Hospital of Jilin University, Changchun 130021, China
[2]Lead contact
*Correspondence: zhengyang@jlu.edu.cn (Y.Z.), caihe19@mails.jlu.edu.cn (H.C.)
https://doi.org/10.1016/j.isci.2024.109134

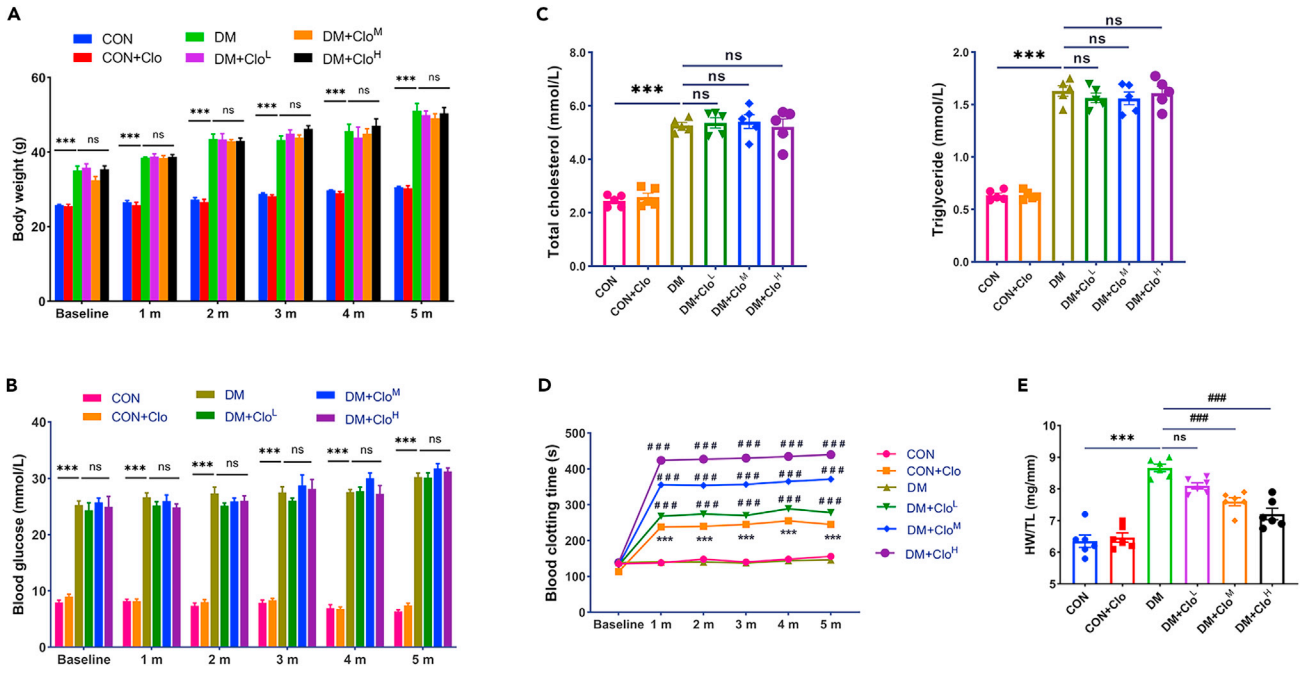

Figure 1. Physical and biochemical characteristics of the mice

(A) Body weight of the mice (n = 6 per group).

(B) Fasting blood glucose levels of the mice (n = 6 per group).

(C) Serum triglyceride and total cholesterol levels of the mice (n = 5 per group).

(D) Blood clotting time of the mice (n = 6 per group).

(E) Heart weight/tibial length ratio (HW/TL) showing the relative heart weight (n = 6 per group). The data are presented as the mean ± SEM. Multiple comparisons were conducted with one-way ANOVA, followed by Tukey's pairwise test. ***p < 0.001 vs. the CON group; ###p < 0.001 vs. the DM group; ns (no significant difference).

RESULTS

Physical and biochemical characteristics of mice and Clo attenuate DM-induced cardiac dysfunction and cardiac hypertrophy

DM mice presented progressive increases in body weight and blood glucose; however, Clo had no significant effect on either variable (Figures 1A and 1B). Additionally, the serum triglyceride and total cholesterol levels in DM mice were significantly elevated but were not decreased by Clo treatment (Figure 1C). The baseline bleeding time did not differ between DM and control (CON) mice, and Clo treatment increased the bleeding time in a dose-dependent manner (Figure 1D), which reflected the effective inhibition of platelet aggregation and the achievement of anticoagulant effects. The heart weight-to-tibial length ratio (HW/TL) increased in DM mice, which was attenuated by Clo treatment (Figure 1E). Cardiac hypertrophy (assessed by the left ventricular posterior wall diastolic thickness [LVPWd] and the size of cardiomyocytes) was also observed in DM mice, and Clo treatment attenuated DM-induced cardiac hypertrophy in a dose-dependent manner (Figures 2A and 2B). Compared with those in CON mice, the cardiac function of DM mice was impaired, as reflected by a reduced left ventricular ejection fraction (EF), left ventricular fractional shortening (FS), and ratio of the E wave to the A wave across the mitral valve (MV E/A ratio), which were reversed by Clo treatment (Figure 2A). Additionally, Clo treatment ameliorated DM-induced left ventricular enlargement (assessed by the left ventricular internal diameter at diastole [LVIDd]) and further improved myocardial remodeling (Figure 2A). As additional markers of cardiac hypertrophy and cardiac function, the protein and mRNA levels of myosin heavy chain 7 (MYH7) and natriuretic peptide type A (ANP) were significantly increased in DM mice, and these increases were prevented by Clo treatment in a dose-dependent manner (Figures 2C and 2D). Consistent with these functional results, Clo prevented the DM-induced increase in the serum lactate dehydrogenase (LDH), creatine kinase (CK), and creatine kinase-myocardial band (CK-MB) levels in DM mice (Figure 2E). Taken together, these results provide clear evidence that Clo treatment could significantly prevent functional cardiac impairment and reverse cardiac hypertrophy caused by diabetes.

Negative correlation between Clo dosage and DM-induced cardiac fibrosis

In addition to cardiac hypertrophy, cardiac fibrosis is a vital effect of cardiac remodeling.[2] First, we evaluated myocardial fibrosis in mice by Masson's trichrome staining and observed severe cardiac fibrosis in DM mice, which was ameliorated by Clo treatment in a dose-dependent

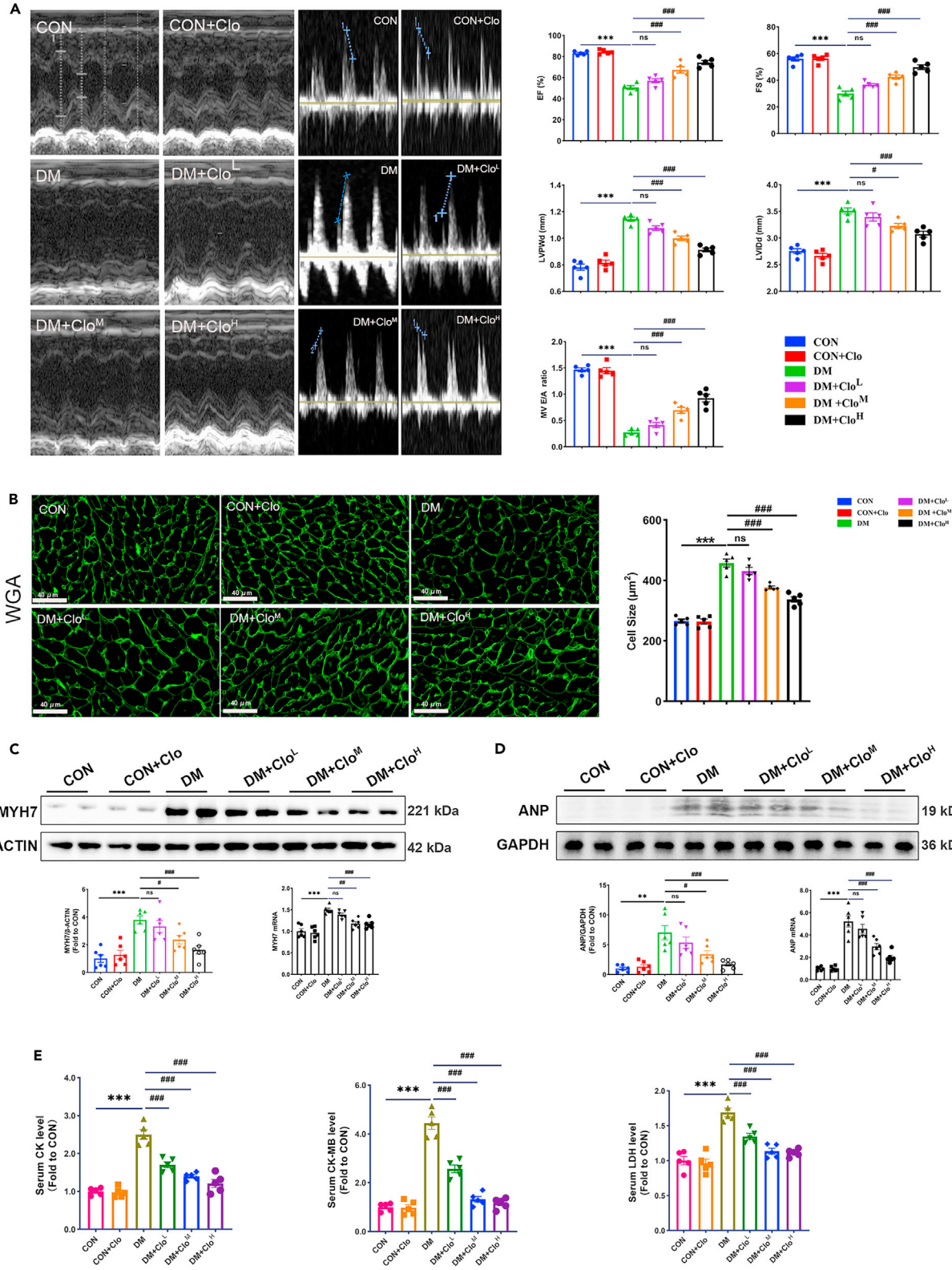
A
CON
CON+Clo
DM
DM+Clo^L
DM+Clo^M
DM+Clo^H
EF (%)
FS (%)
LVPWd (mm)
LVIDd (mm)
MV E/A ratio
B
WGA
Cell Size (μm²)
C
MYH7
β-ACTIN
221 kDa
42 kDa
MYH7/β-ACTIN (Fold to CON)
MYH7 mRNA
D
ANP
GAPDH
19 kDa
36 kDa
ANP/GAPDH (Fold to CON)
ANP mRNA
E
Serum CK level (Fold to CON)
Serum CK-MB level (Fold to CON)
Serum LDH level (Fold to CON)

Figure 2. Clo decreases DM-induced cardiac dysfunction and cardiac hypertrophy

(A) Representative echocardiography and cardiac parameters measured via echocardiography (n = 5 per group).

(B) WGA staining of the cardiac tissue for assessing cardiomyocyte size in cross-sections of the heart (n = 5 per group). Scale bar: 40 μm.

(C) The protein and mRNA expression levels of MYH7 were used to evaluate cardiac hypertrophy (n = 6 per group).

(D) The protein and mRNA expression levels of ANP were used to evaluate cardiac function (n = 6 per group).

(E) Serum LDH, CK, and CK-MB levels in the mice (n = 5 per group). The data are presented as the mean ± SEM. Multiple comparisons were conducted with one-way ANOVA, followed by Tukey's pairwise test. *p < 0.05, **p < 0.01, ***p < 0.001 vs. the CON group; #p < 0.05, ##p < 0.01, ###p < 0.001 vs. the DM group; ns (no significant difference).

manner (Figure 3A). Next, immunohistochemical staining and immunofluorescence analysis were employed, and we observed extensive TGF-β1 deposition concomitant with increased collagen type I alpha 1 chain (COL1A1), Fibronectin, and α-smooth muscle actin (α-SMA) deposition in the cardiac tissues of DM mice; this deposition was suppressed by Clo treatment in a dose-dependent manner (Figure S1). CD90 is a surface marker specific for fibroblasts.[21,22] Based on this, two-color immunofluorescence was used to identify the transition of cardiac fibroblasts to myofibroblasts in mouse cardiac tissue. We observed a significant increase in this transition in DM mice, which was markedly reduced after treatment with Clo (Figure S1B). Upon further examination, we found that the marked increase in both the protein and mRNA expression of α-SMA, COL1A1, collagen type III alpha 1 chain (COL3A1), and Fibronectin in DM mice was abrogated by Clo treatment (Figure 3B). Western blotting and quantitative reverse-transcription PCR (RT-qPCR) also revealed that the significantly elevated protein and mRNA expression levels of fibrotic markers (TGF-β1 and connective tissue growth factor (CTGF)) in DM mice were decreased by Clo treatment in a dose-dependent manner (Figure 3C). These findings demonstrated that Clo could alleviate DM-induced fibrosis by inhibiting TGF-β1 and α-SMA+ myofibroblasts.

The TGF-β1/Smad pathway is involved in Clo-induced decreases in DM-induced cardiac fibrosis

Cardiac fibrosis can be regulated by TGF-β1 through the Smad-dependent signaling pathway (TGF-β1/Smad2/3) and the Smad-independent signaling cascade involving the mitogen-activated protein kinases (MAPKs) c-Jun N-terminal kinase (JNK), P38, and extracellular-signal-regulated kinase (ERK).[9,10,23,24] Therefore, we explored whether Clo treatment could alleviate DM-induced fibrosis through the TGF-β1/Smad and MAPK pathways. Our results revealed that, in comparison with those in the CON group, Smad3 and Smad2 phosphorylation was elevated in the DM group, and this phosphorylation was abrogated by Clo treatment (Figure 4A). Additionally, a previous study revealed that Smad3 acts as a transcription factor that increases P2RY12 expression by binding to its promoter.[14] In our study, both the protein and mRNA levels of P2RY12 were significantly elevated in the DM group, and Clo treatment attenuated these changes in DM mice (Figure 4B). These results indicated that Clo treatment could effectively block the TGF-β1/Smad3/P2RY12 pathway in DM mice.

The MAPK signaling pathway was also evaluated at the protein level in the present study. The results indicated that the ERK, JNK, and p38 signaling pathways were activated in DM mice and that Clo treatment suppressed ERK and JNK phosphorylation. However, Clo had no significant effect on P38 signaling in DM mice (Figure 4C).

Taken together, these results demonstrated that Clo alleviates cardiac fibrosis in DCM by inhibiting the TGF-β1/Smad, ERK, and JNK pathways.

Reduced DM-induced cardiac macrophage infiltration and cardiac inflammatory responses are implicated in Clo effectiveness

In DCM, inflammatory responses can contribute to cardiac dysfunction and remodeling. Previous studies revealed macrophage infiltration and the overexpression of inflammatory cytokines in diabetic hearts.[9,25] P2RY12 has been found on the surface of macrophages and platelets, and therapies targeting P2RY12 reduce the infiltration of these cells.[14,17]

F4/80 is a surface marker specific for macrophages. Immunofluorescence analysis was used to measure F4/80 levels in mouse myocardial tissue. Macrophage infiltration was significantly increased in DM mice, and this infiltration was decreased by medium to high doses of Clo treatment (Figure 5A). The anti-inflammatory effects of Clo were further confirmed by evaluating inflammatory cytokines. We observed that the protein and mRNA expression levels of tumor necrosis factor α (TNF-α), interleukin 1 beta (IL-1β), and interleukin 6 (IL-6) were increased in DM mice, and these effects were reduced by medium to high doses of Clo (Figure 5B). C-C motif chemokine ligand 2 (known as MCP-1), intercellular adhesion molecule 1 (ICAM1), and vascular cell adhesion molecule 1 (VCAM1) also contribute to the progression of DCM, prompting us to assess their expression. The marked increase in MCP-1, ICAM1, and VCAM1 protein and mRNA expression in DM mice was decreased by medium to high doses of Clo (Figure 5C). Conversely, low-dose Clo treatment had no effect on the upregulation of TNF-α, IL-1β, IL-6, MCP-1, ICAM1, or VCAM1 at either the protein or mRNA level in DM mice. This finding suggested that an increase in the Clo dosage is necessary to mitigate inflammatory responses.

We also evaluated the effects of Clo on the serum levels of TNF-α, IL-1β, IL-6, and MCP-1 in mice by enzyme-linked immunosorbent assay (ELISA) (Figure 5D). The presence of these inflammatory cytokines in the serum can reflects systemic inflammation. The results indicated that the serum TNF-α, IL-1β, IL-6, and MCP-1 levels were markedly increased in diabetic mice, and these increases were suppressed by Clo treatment.

These results demonstrated that Clo could attenuate DM-induced macrophage infiltration and reduce the secretion of inflammatory cytokines and adhesion molecules by blocking P2RY12, thereby protecting the heart against inflammatory response-induced damage.

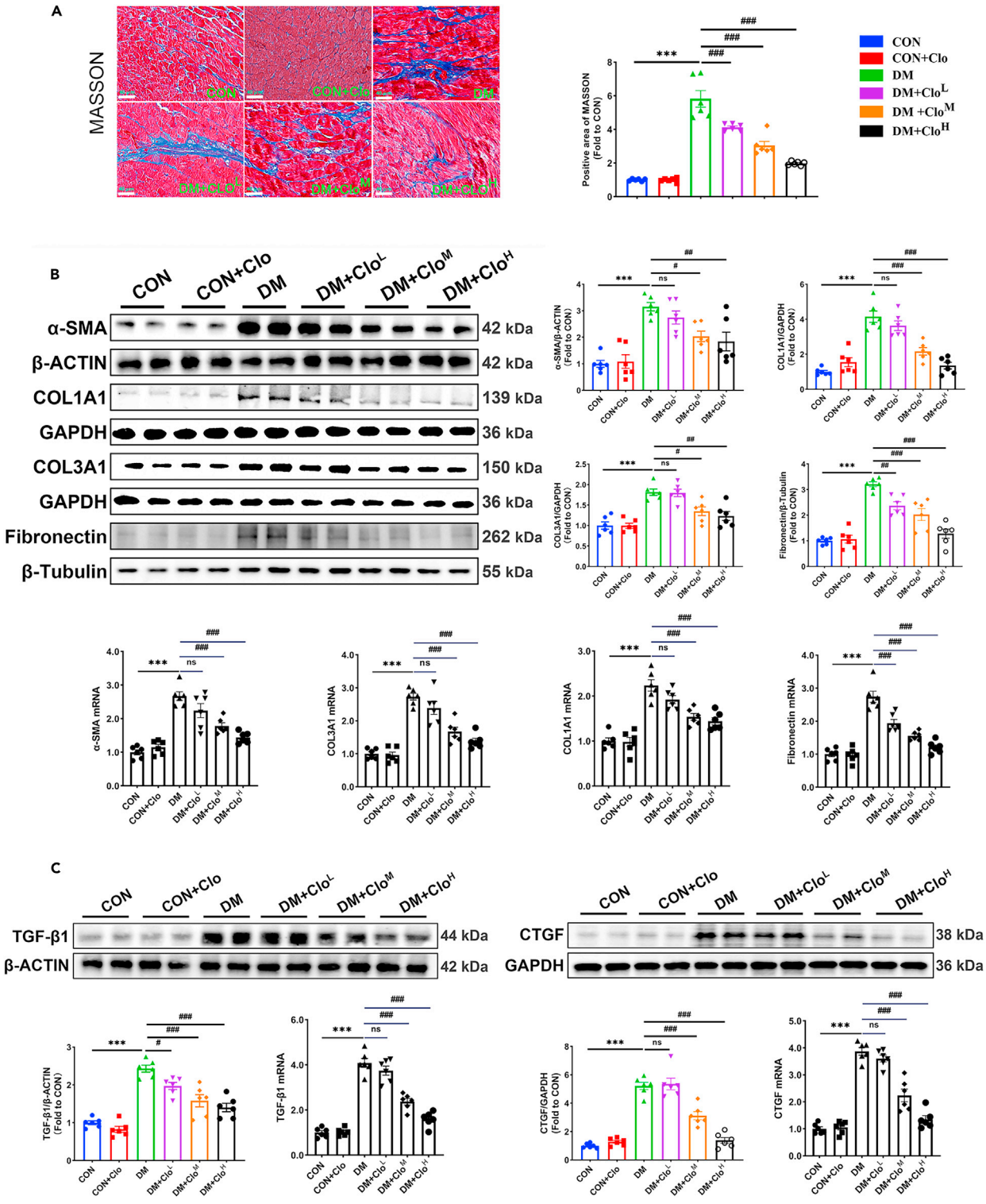

Figure 3. Negative correlation between Clo dosage and DM-induced cardiac fibrosis

(A) Representative images of Masson's trichrome staining followed by quantification of the percent positive area (n = 6 per group). Scale bar: 40 μm.

(B) Western blotting and RT-qPCR analysis of α-SMA, COL1A1, COL3A1, and Fibronectin, and quantitation of their expression (n = 6 per group).

(C) TGF-β1 and CTGF were analyzed using western blotting and RT-qPCR (n = 6 per group). The data are presented as the mean ± SEM. Multiple comparisons were conducted with one-way ANOVA, followed by Tukey's pairwise test. ***p < 0.001 vs. the CON group; #p < 0.05, ##p < 0.01, ###p < 0.001 vs. the DM group; ns (no significant difference).

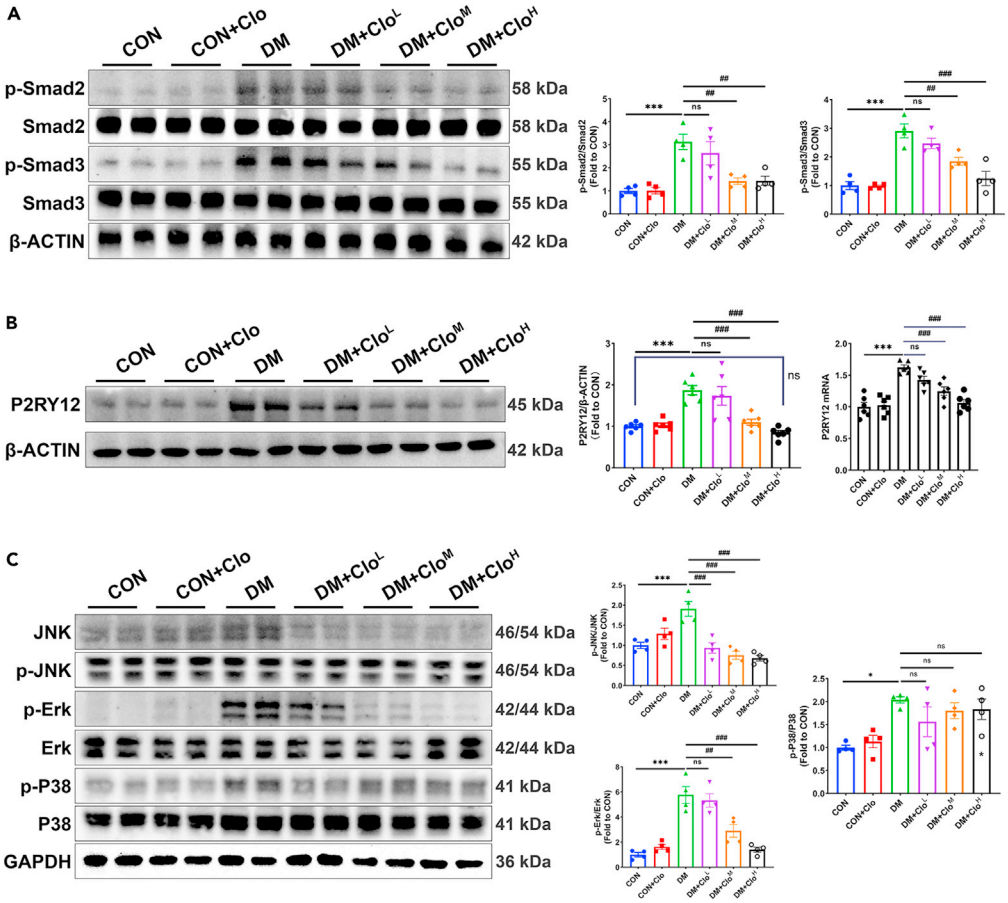

Figure 4. The TGF-β1/Smad pathway is involved in Clo-induced decreases in DM-induced cardiac fibrosis

(A) The levels of *p*-Smad2, Smad2, *p*-Smad3, and Smad3 were analyzed via western blotting, and the ratios of *p*-Smad2 to Smad2 and *p*-Smad3 to Smad3 were quantified (n = 4 per group).

(B) P2RY12 was analyzed using western blotting and RT-qPCR (n = 6 per group).

(C) Western blotting of ERK, *p*-ERK, JNK, *p*-JNK, P38, and p-P38 and quantitative analysis of the ratios of *p*-ERK to ERK, *p*-JNK to JNK, and p-P38 to P38 (n = 4 per group). The data are presented as the mean ± SEM. Multiple comparisons were conducted with one-way ANOVA, followed by Tukey's pairwise test. *p < 0.05, **p < 0.01, ***p < 0.001 vs. the CON group; #p < 0.05, ##p < 0.01, ###p < 0.001 vs. the DM group; ns (no significant difference).

Clo-induced Nrf2 pathway activation prevents DM-induced cardiac oxidative stress damage

Extensive evidence indicates that ROS accumulation can lead to cardiac fibrosis by facilitating the production and activation of TGF-β and promoting the differentiation of cardiac fibroblasts into myofibroblasts.[26,27] Western blotting revealed a significant increase in Kelch-like ECH-associated protein 1 (Keap1) expression, whereas nuclear Nrf2 (nNrf2) protein expression was significantly reduced in mice with DM (Figure 6A). Clo treatment increased nNrf2 expression and decreased Keap1 protein expression in DM mice. In addition, the expression of downstream proteins of Nrf2, including oxygenase 1 (HO-1), NAD(P)H quinone dehydrogenase 1 (NQO-1), and catalase (CAT), was also repressed in the cardiac tissues of DM mice, and Clo treatment reversed this repression (Figure 6A). The mRNA expression changes of Nrf2, HO-1, NQO-1, and CAT are consistent with their protein levels (Figure 6B).

We also evaluated the effects of Clo on DM-induced oxidative stress in mouse heart tissue. The levels of superoxide dismutase (SOD), CAT, and glutathione (GSH) in the heart were markedly reduced in the DM group, and these changes were alleviated by Clo treatment (Figure 6C). Additionally, the markedly elevated levels of malondialdehyde (MDA) and 3-nitrotyrosine (3-NT) in the DM mice were decreased by Clo treatment (Figure 6C).

Clo treatment ameliorates glucolipotoxicity-induced cardiac hypertrophic responses and oxidative stress in AC16 cells

Initially, we assessed the viability of AC16 cells stimulated with 33 mM high glucose (HG) and increasing concentrations of palmitic acid (PA) using the Cell Counting Kit-8 (CCK-8) method. The half maximal inhibitory concentration of PA treatment in AC16 cells ranged from 300 μM to 400 μM (Figure S2A). Therefore, we selected a PA concentration of 300 μM and an HG concentration of 33 mM to establish a type-2 diabetes

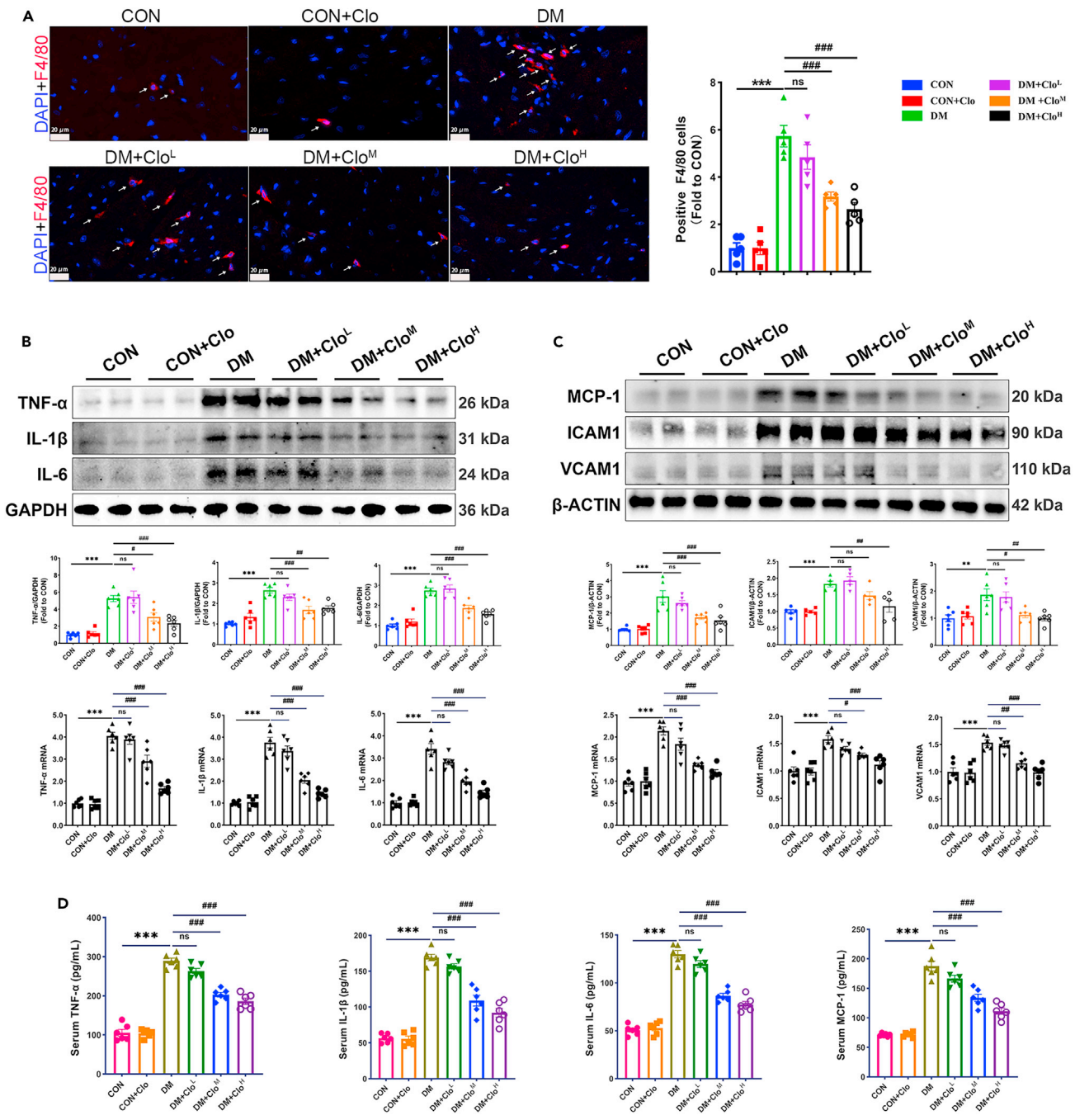

Figure 5. Reduced DM-induced cardiac macrophage infiltration and cardiac inflammatory responses are implicated in Clo effectiveness

(A) Representative fluorescence images of F4/80 and quantification of F4/80 expression. The white arrows indicate F4/80-positive cells (n = 5 per group). Scale bar: 20 μm.

(B) Western blotting and mRNA expression of TNF-α, IL-1β, and IL-6 (n = 6 per group).

(C) Western blotting and mRNA levels of MCP-1, ICAM1, and VCAM1 (n = 5–6 per group).

(D) Serum levels of TNF-α, IL-1β, IL-6, and MCP-1 in mice (n = 6 per group). The data are presented as the mean ± SEM. Multiple comparisons were conducted with one-way ANOVA, followed by Tukey's pairwise test. *p < 0.05, **p < 0.01, ***p < 0.001 vs. the CON group; #p < 0.05, ##p < 0.01, ###p < 0.001 vs. the DM group; ns (no significant difference).

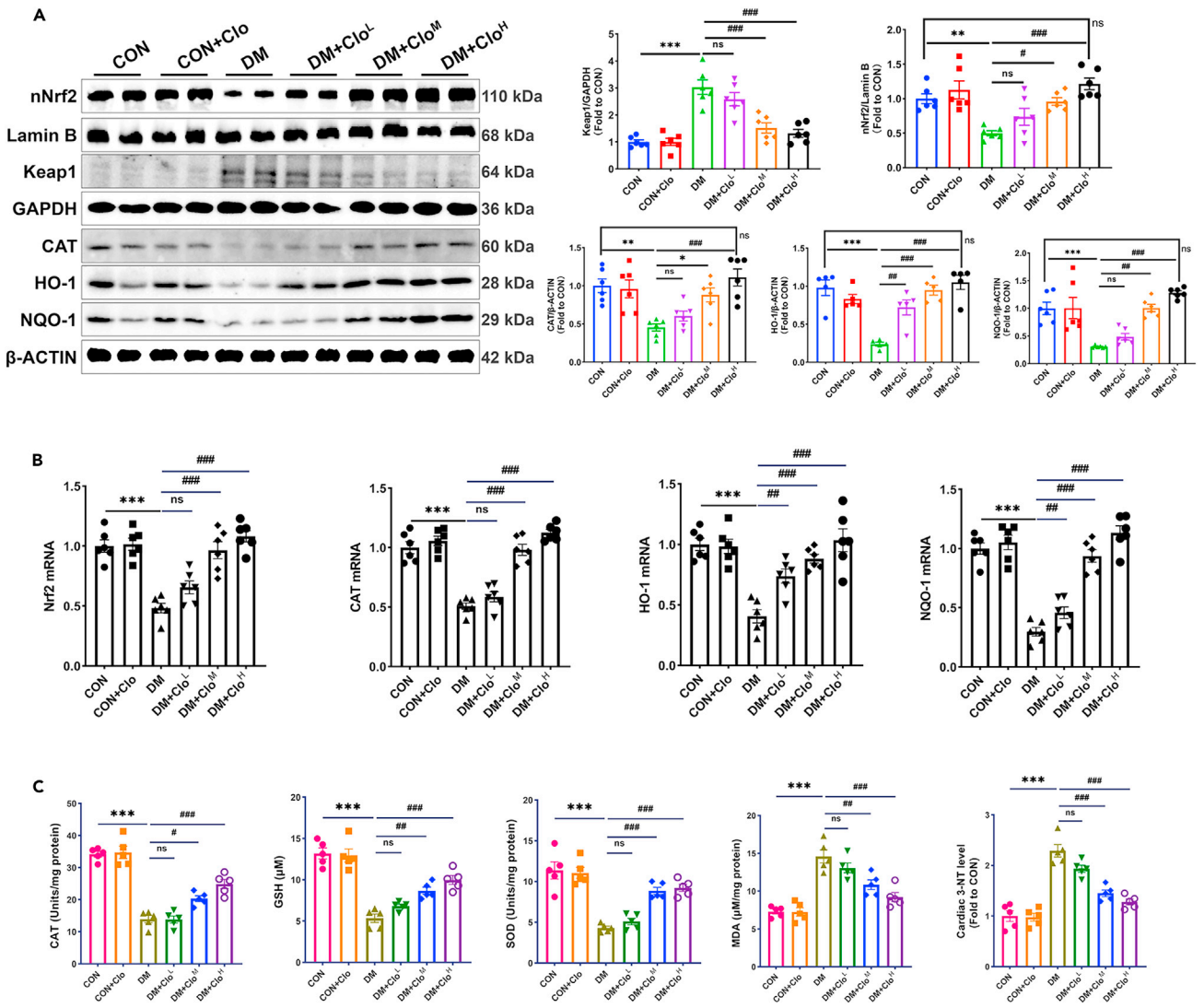

Figure 6. Clo-induced Nrf2 pathway activation prevents DM-induced cardiac oxidative stress damage

(A) Western blotting and quantitative analysis of nuclear Nrf2 (nNrf2), Keap1, CAT, HO-1, and NQO-1 (n = 5–6 per group).

(B) RT-qPCR and quantitative analysis of Nrf2, CAT, HO-1, and NQO-1 expression (n = 6 per group).

(C) The levels of SOD, CAT, GSH, MDA, and 3-NT in heart tissues (n = 5 per group). The data are presented as the mean ± SEM. Multiple comparisons were conducted with one-way ANOVA, followed by Tukey's pairwise test. *p < 0.05, **p < 0.01, ***p < 0.001 vs. the CON group; #p < 0.05, ##p < 0.01, ###p < 0.001 vs. the DM group; ns (no significant difference).

cell model. Subsequently, the CCK-8 method was used to assess the viability of AC16 cells after exposure to varying concentrations of Clo (ranging from 0 to 100 μM). No significant differences in cell viability were observed (Figure S2B). RT-qPCR was used to assess the mRNA expression of Nrf2 in AC16 cells after treatment with various concentrations of Clo (ranging from 0 to 50 μM) for 24 h; when the Clo concentration was greater than 10 μM, the mRNA expression of Nrf2 in AC16 cells was significantly increased (Figure S3). Based on our findings and those of previous studies,[14,16] we selected a concentration of 10 μM Clo for further assessment of its impact on diabetes-induced cellular damage.

As shown in Figure S4A, the size of cardiomyocytes induced by glucolipotoxicity was significantly larger than that in the negative control (NC) group. However, treatment with Clo attenuated the glucolipotoxicity-induced cardiac hypertrophy. Additionally, we observed that the protein levels of MYH7 and ANP were significantly increased in the PA + HG group, and these increases were prevented by Clo treatment (Figure S4B). The ROS level in the PA + HG group was significantly elevated, and this increase was alleviated by Clo treatment (Figure S4C). Further examination revealed that the markedly decreased protein levels of Nrf2, HO-1, and NQO-1 in the PA + HG group were elevated by Clo treatment (Figure S4D).

DISCUSSION

To date, emerging evidence has highlighted the critical roles of the inflammatory response, ROS, and cardiac fibrosis in the development of DCM.[2,7,9,10] Clo, an oral antiplatelet drug that irreversibly binds to P2RY12, confers various biological benefits, including anti-inflammatory, antioxidant, and antifibrotic effects.[14–17] Consequently, this study investigated the potential of Clo to prevent DCM in db/db mice and elucidated the underlying mechanism involved. These results demonstrated that Clo mitigated DM-induced cardiac dysfunction and hypertrophy; alleviated cardiac fibrosis by inhibiting the TGF-β/Smad pathway, macrophage infiltration, and inflammatory responses; and reduced cardiac ROS accumulation through activation of the Nrf2 pathway.

In our investigation, the increased dosage of Clo (20 mg/kg/day per mouse) surpassed the recognized standard human treatment threshold of 75 mg. The selection of the higher dosage in our study was informed by prior investigations in murine models.[20,28] These studies demonstrated that 5 mg/kg/day Clo effectively suppressed angiotensin II-induced vascular remodeling in mice, while 20 mg/kg/day Clo improved diabetes-induced renal fibrosis. Accordingly, our study employed these escalating doses (5/10/20 mg/kg/day) of Clo to explore their effects on DCM. Additionally, it has been reported that 60 mg/kg/day of Clo has been used to explore its effects on renal fibrosis.[14] The study demonstrated that Clo treatment inhibits unilateral ureteral obstruction-induced renal fibrosis in a dose-dependent manner, with the most effective dose identified as 60 mg/kg/day. Moreover, the translation of dosages from animal models to humans involves complex factors such as metabolic rate, bioavailability, and species-specific responses. The purpose of our study was not to establish a direct correlation between animal dosage and human therapeutic dose but rather to examine the potential protective effects of Clo across a range of concentrations. Additionally, these studies indicated that the effective dosage of Clo varies across different mouse disease models and that the effect of Clo may increase with increasing dosage. This observation highlights the dose-dependent effect of Clo in mouse disease models, providing valuable insights into the biological effects and mechanisms of Clo. However, it is challenging to balance the bleeding risk associated with high doses of Clo. Therefore, in our study, based on previous research, we selected a dose range that has been reported to be safe. Additionally, we conducted a specific examination of blood clotting time after treatment with various doses of Clo. The results indicated that, as the dose of Clo increased, the blood clotting time tended to increase. We consider this experimental outcome to be a crucial indicator of the correlation between Clo dosage and bleeding risk. Thus, in the DM-induced DCM model in db/db mice, the effectiveness of Clo in improving myocardial fibrosis in diabetic mice increased with higher doses, particularly within the range of 5–20 mg/kg/day.

Cardiac fibrosis is an important hallmark of DCM, and ECM generation is a key marker of cardiac fibrosis. Cardiac fibrosis is mediated mainly by cardiac fibroblasts, which are abundant in the myocardium and are normally in an inactive state. Following cardiac injury, cardiac fibroblasts undergo differentiation into contractile myofibroblasts.[13,29] Furthermore, differentiation of fibroblasts to myofibroblasts can be triggered by various cytokines, including TGF-β and platelet-derived growth factor (PDGF), which are secreted by immune cells.[24,30] In addition to resident cardiac fibroblasts, cells derived from epithelial and endothelial origins can undergo a transition to a myofibroblast phenotype through epithelial-to-mesenchymal transition and endothelial-to-mesenchymal transition, respectively. This process is regulated by growth factors, including fibroblast growth factor and PDGF.[13,31–33] These transformed cells with a myofibroblast phenotype and myofibroblasts are characterized by the expression of contractile protein such as α-SMA and the secretion of large amounts of ECM. The components of the ECM include collagen, elastin, fibronectin, and laminin, among which collagen deposition (especially that of type-I and type-III collagens) is a vital feature of cardiac fibrosis.[13] ECM deposition results in heightened cardiac stiffness and diminished ventricular compliance, subsequently compromising the normal diastolic and systolic functions of the heart and ultimately contributing to heart failure. In our study, we observed excessive deposition of ECM components, such as collagen I, collagen III, and fibronectin, in the cardiac tissue of diabetic mice, and this ECM deposition was decreased by Clo treatment. We additionally noted substantial activation of α-SMA+ myofibroblasts, coinciding with an increase in TGF-β1 in the cardiac tissue of diabetic mice, and these changes were reversed by Clo treatment. These results illustrated that Clo could alleviate cardiac fibrosis induced by α-SMA+ myofibroblasts via blocking TGF-β1 in DM mice. Despite robust evidence supporting the central role of TGF-β in driving collagen gene expression and the complete inhibition of organ fibrosis by TGF-β inhibition alone,[24] it is imperative to elucidate the mechanism through which Clo inhibits cardiac fibrosis via the TGF-β1 pathway. Accordingly, we assessed both Smad-dependent and Smad-independent signaling pathways. Substantial evidence suggests that inhibiting the TGF-β1/Smad3 pathway can mitigate myocardial fibrosis in diabetic mice.[34,35] Consistent with these findings, we found that Clo alleviated cardiac fibrosis in DCM by inhibiting the TGF-β1/Smad3 signaling pathway. Additionally, the ERK, JNK, and p38 signaling pathways were activated in the cardiac tissue of diabetic mice, and Clo treatment suppressed the phosphorylation of ERK and JNK. However, Clo had no effect on P38 signaling in the cardiac tissue of diabetic mice. Prior research has demonstrated that Smad3 functions as a transcription factor, enhancing P2RY12 expression by binding to its promoter.[14] Extensive evidence has demonstrated that treatment with Clo, known for its P2RY12 inhibitory effects, impedes the release of inflammatory markers that facilitate myocardial remodeling.[17,18] Additionally, knockout of the P2RY12 gene in mice alleviated cardiac remodeling and enhanced cardiac function.[17] In our study, the expression of the P2RY12 protein increased concurrently with the increase in the TGF-β1 and *p*-Smad3 levels in diabetic hearts, and Clo treatment mitigated the DM-induced upregulation of P2RY12. Therefore, we deduced that P2RY12 is involved in the TGF-β1/Smad3/P2RY12 signaling cascade in DCM.

Another crucial aspect of the pathogenesis of DCM involves a substantial increase in macrophage infiltration and the overexpression of inflammatory cytokines in diabetic hearts.[7,9,25] Our study revealed an increase in macrophage infiltration in the heart of diabetic mice, and Clo treatment effectively mitigated this increase. A heightened abundance of macrophages can induce cardiac fibrosis either by activating cardiac fibroblasts or through the acquisition of a fibrogenic phenotype following cardiac injury.[12,36,37] Additionally, these cells contribute to ventricular fibrosis and provoke inflammatory responses in the heart by releasing various fibrogenic mediators[12] and inflammatory cytokines, including TNF-α, IL-1β, and IL-6. Prolonged hyperglycaemia additionally elevates the levels of inflammatory cytokines (TNF-α, IL-1β, and IL-6),

MCP-1, and cell adhesion molecules (ICAM1 and VCAM1) in diabetic hearts.[7,9] In addition, TNF-α indirectly regulates the expression of ICAM1 and VCAM1. Consequently, these increased inflammatory responses expedite structural and functional deterioration in the diabetic heart.

Our findings demonstrated that the onset of diabetes led to significant elevations in the protein levels of TNF-α, IL-1β, IL-6, MCP-1, ICAM1, and VCAM1 in the diabetic heart, all of which were mitigated by Clo treatment. These findings suggest that Clo treatment attenuates diabetes-induced macrophage infiltration and reduces the secretion of inflammatory cytokines and adhesion molecules, thereby protecting the heart from damage associated with the inflammatory response. Moreover, P2RY12 has been identified on the surface of macrophages, and therapies directed at P2RY12 have been shown to diminish macrophage infiltration.[14,17] Patients with diabetes exhibit heightened platelet activity, and the platelet P2RY12 level is four times greater in individuals with T2DM than in their healthy counterparts.[38] Previous studies have shown that TGF-β can also be produced by macrophages, parenchymal cells (such as fibroblasts), and platelets during tissue repair,[26,39] and the function of TGF-β can be enhanced by PDGF. In addition, upon its release from activated platelets, PDGF significantly contributes to fibroblast-to-myofibroblast differentiation, and therapies targeting PDGF have been shown to inhibit fibrosis.[24,39] Thus, we inferred that Clo could inhibit α-SMA+ myofibroblast-driven fibrosis by suppressing platelet activation and the subsequent secretion of PDGF and TGF-β1. Additionally, the inhibition of the TGF-β/Smad/P2RY12/macrophage pathway is implicated in cardiac fibrosis and cardiac inflammatory responses.

ROS are considered primary instigators of DCM. Earlier investigations have shown that elevated ROS levels induced by hyperglycaemia contribute to both cardiac dysfunction and fibrosis in diabetic rats.[11,12] The Nrf2 pathway and its downstream genes play crucial roles in providing substantial protection against DCM associated with ROS-induced injury. A previous study from our research group demonstrated that activating the Nrf2 signaling pathway ameliorated cardiac fibrosis in DCM.[7] Furthermore, an additional study reported that Clo exhibits antioxidant and anti-inflammatory effects through the activation of Nrf2 signaling.[16] In the present study, the protein expression of nNrf2 and its downstream proteins, such as HO-1, NQO-1, and CAT, was suppressed in the cardiac tissue of diabetic mice, whereas Clo treatment reversed this repression, thereby enhancing antioxidant activity. Substantial evidence indicates that the accumulation of ROS can contribute to cardiac fibrosis by facilitating the production and activation of TGF-β and promoting the differentiation of cardiac fibroblasts into myofibroblasts.[26,27] The accumulation of ROS promotes the phosphorylation of the TGF-β receptor, thereby activating downstream signaling even in the absence of TGF-β.[39] Treatment targeting the Nrf2 pathway attenuates cardiac fibrosis by inhibiting cardiac fibroblast activation and proliferation.[27] Therefore, we hypothesized that Clo treatment attenuated diabetes-induced ROS accumulation by activating the Nrf2 pathway, further inhibiting TGF-β. Based on our study, we observed a trend suggesting that high-dose Clo treatment may be more effective in diabetic mice than it is in normal mice. This is supported by higher levels of Nrf2, CAT, HO-1, and NQO-1 in the high-dose Clo group compared to the normal control group. However, it is crucial to note that this observed trend was not statistically significant. In addition, in our *in vitro* experiments, RT-qPCR was used to evaluate the mRNA expression of Nrf2 in AC16 cells after exposure to varying concentrations of Clo. Our findings revealed a positive correlation between the concentration of Clo and the upregulation of Nrf2 mRNA expression. Consequently, to delve deeper into the comparison of high-dose Clo treatment effectiveness versus normal mice, an assessment of the protective effects of higher Clo doses (40 mg/kg/day, 60 mg/kg/day) on DCM in diabetic mice is warranted.

DM has a substantial global burden, affecting more than 0.5 billion adults globally.[40] DCM and coronary heart disease are considered critical cardiovascular complications associated with diabetes. Clo has been widely applied in the treatment of coronary heart disease, and it significantly decreases cardiovascular events in patients with T2DM.[41] Our findings indicate that Clo protects against DCM by preventing cardiac fibrosis and dysfunction, providing robust evidence supporting its use in the primary and secondary prevention of cardiovascular events in high-risk patients with diabetes.

In summary, Clo ameliorates cardiac fibrosis through its influence on various cardiac cell types, including platelets, cardiac fibroblasts, and macrophages. Cardiac fibroblasts play a pivotal role in cardiac fibrosis by transforming into myofibroblasts and synthesizing and secreting ECM, thereby inducing fibrosis and stiffening of cardiac tissue. As an antiplatelet medication, Clo acts by irreversibly binding to P2RY12 on platelets. By regulating the secretion of PDGF and TGF-β1 from platelets, Clo modulates the activity of cardiac fibroblasts. This regulatory effect inhibits the differentiation of cardiac fibroblasts into myofibroblasts, thereby mitigating their contribution to cardiac fibrosis. Additionally, emerging evidence indicates that P2RY12 is not exclusive to platelets but is also present on the surface of macrophages. The ability of macrophages to induce cardiac fibrosis by either activating fibroblasts or acquiring a fibrogenic phenotype following cardiac injury can be influenced by therapies targeting P2RY12. Treatment directed at P2RY12 has been shown to reduce macrophage infiltration, thereby further supporting the role of Clo in ameliorating cardiac fibrosis through its impact on macrophages. This study provides valuable insights into the potential therapeutic mechanisms of Clo in mitigating cardiac fibrosis, offering a promising avenue for the treatment of cardiovascular complications.

Conclusions

In summary, our findings suggested that Clo protects against DCM by inhibiting cardiac fibrosis, inflammatory responses, and oxidative stress in db/db mice. The mechanism of this protective effect involves the inhibition of TGF-β1/Smad3/P2RY12 signaling, the suppression of macrophage infiltration, and the activation of the Nrf2 signaling pathway (Figure 7). Furthermore, Clo is expected to be an effective treatment for DCM, especially in patients with diabetes complicated by coronary heart disease.

Limitations of the study

Our study has several limitations. First, we inferred that Clo might inhibit α-SMA+ myofibroblast-driven fibrosis by reducing platelet activation and the subsequent secretion of PDGF and TGF-β1, but PDGF expression and the degree of platelet activation were not evaluated in our

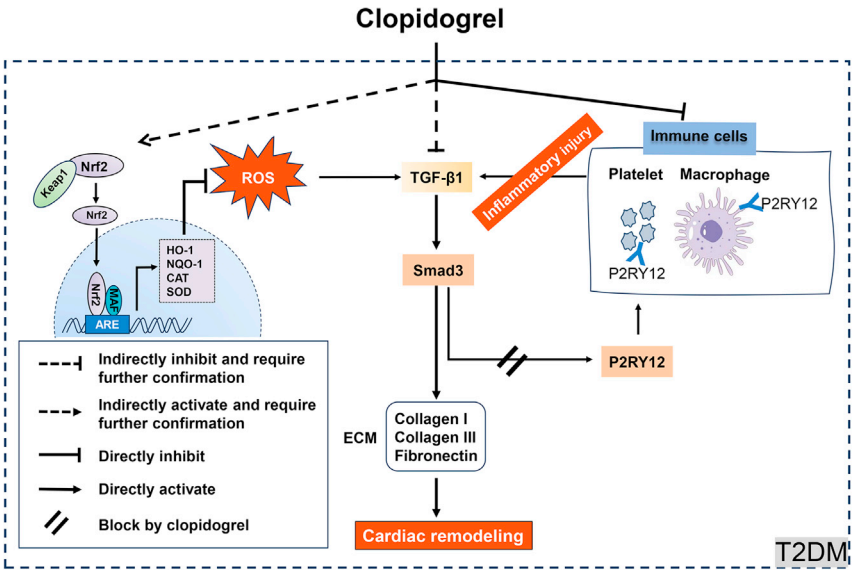

Figure 7. Mechanism for the protective effects of clopidogrel on DCM

T2DM-induced inflammatory responses, ROS accumulation, and cardiac fibrosis are hallmark mediators of DCM development. Clopidogrel attenuates DM-induced ROS accumulation by activating Nrf2 and its downstream effects (HO-1, NQO-1, SOD, and CAT). Clopidogrel attenuated the DM-induced increase in macrophage infiltration and hyperactive platelets by inhibiting P2RY12. Along these lines, the DM-induced increase in the expression of TGF-β1, which is partly secreted by macrophages and platelets, was inhibited by clopidogrel treatment. Diabetes-induced cardiac fibrosis can be alleviated by clopidogrel treatment via repression of the TGF-β1/Smad3/P2RY12 pathway.

study. Second, a critical limitation of our study is the lack of validation or assessment of the proposed mechanism in cardiac fibroblasts. We plan to conduct pertinent experiments in future research to investigate the action of Clo at the cardiac fibroblast level, thereby providing a more comprehensive understanding of the underlying mechanisms involved. Third, our experimental results demonstrate a protective effect of Clo against T2DM-induced DCM in mice. However, there is currently a lack of relevant clinical population data. Therefore, before directly applying it to clinical practice, further evaluation is needed to assess the performance of Clo in terms of dosage safety and efficacy.

STAR★METHODS

Detailed methods are provided in the online version of this paper and include the following:

- KEY RESOURCES TABLE
- RESOURCE AVAILABILITY
  - Lead contact
  - Materials availability
  - Data and code availability
- EXPERIMENTAL MODEL AND STUDY PARTICIPANT DETAILS
  - Mouse models
  - Cell lines and cell culture
- METHOD DETAILS
  - Echocardiography
  - Blood glucose levels and blood clotting times
  - Measurement of serum lipid levels in mice
  - Measurement of inflammatory marker levels in serum
  - Evaluation of cardiac marker levels in serum
  - Assessment of oxidative stress
  - Histology
  - Immunohistochemistry
  - Immunofluorescence
  - WGA staining
  - Nuclear protein extraction
  - Western blotting

- Real-time qPCR
- Cell viability assay
- Rhodamine-phalloidin staining
- ROS levels in the cells

- QUANTIFICATION AND STATISTICAL ANALYSIS

SUPPLEMENTAL INFORMATION

Supplemental information can be found online at https://doi.org/10.1016/j.isci.2024.109134.

ACKNOWLEDGMENTS

We thank Zongyu Zheng, PhD, from The First Hospital of Jilin University for providing us with the mice. We thank Mengmeng Li for guiding our figure processing. We thank the editors at AJE for editing the English text of this manuscript.

AUTHOR CONTRIBUTIONS

H.C. and Y. Zheng provided concepts. B.L. performed the experiments and wrote the manuscript. Y. Zhang collected and analyzed the data. H.C. and Y. Zheng revised the manuscript and supervised the experiments.

DECLARATION OF INTERESTS

The authors declare no competing interests.

Received: September 27, 2023
Revised: December 19, 2023
Accepted: February 1, 2024
Published: February 5, 2024

REFERENCES

1. Mortada, I. (2017). Hyperuricemia, Type 2 Diabetes Mellitus, and Hypertension: an Emerging Association. Curr. Hypertens. Rep. *19*, 69. https://doi.org/10.1007/s11906-017-0770-x.
2. Hu, X., Bai, T., Xu, Z., Liu, Q., Zheng, Y., and Cai, L. (2017). Pathophysiological Fundamentals of Diabetic Cardiomyopathy. Compr. Physiol. *7*, 693–711. https://doi.org/10.1002/cphy.c160021.
3. Palmer, A.K., Gustafson, B., Kirkland, J.L., and Smith, U. (2019). Cellular senescence: at the nexus between ageing and diabetes. Diabetologia *62*, 1835–1841. https://doi.org/10.1007/s00125-019-4934-x.
4. Saeedi, P., Petersohn, I., Salpea, P., Malanda, B., Karuranga, S., Unwin, N., Colagiuri, S., Guariguata, L., Motala, A.A., Ogurtsova, K., et al. (2019). Global and regional diabetes prevalence estimates for 2019 and projections for 2030 and 2045: Results from the International Diabetes Federation Diabetes Atlas, 9 (th) edition. Diabetes Res. Clin. Pract. *157*, 107843. https://doi.org/10.1016/j.diabres.2019.107843.
5. Rubler, S., Dlugash, J., Yuceoglu, Y.Z., Kumral, T., Branwood, A.W., and Grishman, A. (1972). New type of cardiomyopathy associated with diabetic glomerulosclerosis. Am. J. Cardiol. *30*, 595–602. https://doi.org/10.1016/0002-9149(72)90595-4.
6. Dillmann, W.H. (2019). Diabetic Cardiomyopathy. Circ. Res. *124*, 1160–1162. https://doi.org/10.1161/circresaha.118.314665.
7. Hu, X., Rajesh, M., Zhang, J., Zhou, S., Wang, S., Sun, J., Tan, Y., Zheng, Y., and Cai, L. (2018). Protection by dimethyl fumarate against diabetic cardiomyopathy in type 1 diabetic mice likely via activation of nuclear factor erythroid-2 related factor 2. Toxicol. Lett. *287*, 131–141. https://doi.org/10.1016/j.toxlet.2018.01.020.
8. Sun, Y., Zhou, S., Guo, H., Zhang, J., Ma, T., Zheng, Y., Zhang, Z., and Cai, L. (2020). Protective effects of sulforaphane on type 2 diabetes-induced cardiomyopathy via AMPK-mediated activation of lipid metabolic pathways and NRF2 function. Metabolism. *102*, 154002. https://doi.org/10.1016/j.metabol.2019.154002.
9. Gu, X., Shi, Y., Chen, X., Sun, Z., Luo, W., Hu, X., Jin, G., You, S., Qian, Y., Wu, W., et al. (2020). Isoliquiritigenin attenuates diabetic cardiomyopathy via inhibition of hyperglycemia-induced inflammatory response and oxidative stress. Phytomedicine. *78*, 153319. https://doi.org/10.1016/j.phymed.2020.153319.
10. Wang, Y., Yu, K., Zhao, C., Zhou, L., Cheng, J., Wang, D.W., and Zhao, C. (2021). Follistatin Attenuates Myocardial Fibrosis in Diabetic Cardiomyopathy via the TGF-β-Smad3 Pathway. Front. Pharmacol. *12*, 683335. https://doi.org/10.3389/fphar.2021.683335.
11. Wilson, A.J., Gill, E.K., Abudalo, R.A., Edgar, K.S., Watson, C.J., and Grieve, D.J. (2018). Reactive oxygen species signalling in the diabetic heart: emerging prospect for therapeutic targeting. Heart *104*, 293–299. https://doi.org/10.1136/heartjnl-2017-311448.
12. Russo, I., and Frangogiannis, N.G. (2016). Diabetes-associated cardiac fibrosis: Cellular effectors, molecular mechanisms and therapeutic opportunities. J. Mol. Cell. Cardiol. *90*, 84–93. https://doi.org/10.1016/j.yjmcc.2015.12.011.
13. Liu, M., López de Juan Abad, B., and Cheng, K. (2021). Cardiac fibrosis: Myofibroblast-mediated pathological regulation and drug delivery strategies. Adv. Drug Deliv. Rev. *173*, 504–519. https://doi.org/10.1016/j.addr.2021.03.021.
14. Chen, J., Tang, Y., Zhong, Y., Wei, B., Huang, X.R., Tang, P.M.K., Xu, A., and Lan, H.Y. (2022). P2Y12 inhibitor clopidogrel inhibits renal fibrosis by blocking macrophage-to-myofibroblast transition. Mol. Ther. *30*, 3017–3033. https://doi.org/10.1016/j.ymthe.2022.06.019.
15. Hadi, N.R., Mohammad, B.I., Ajeena, I.M., and Sahib, H.H. (2013). Antiatherosclerotic potential of clopidogrel: antioxidant and anti-inflammatory approaches. Biomed Res. Int. *2013*, 790263. https://doi.org/10.1155/2013/790263.
16. Yang, H., Zhao, P., and Tian, S. (2016). Clopidogrel Protects Endothelium by Hindering TNFα-Induced VCAM-1 Expression through CaMKKβ/AMPK/Nrf2 Pathway. J. Diabetes Res. *2016*, 9128050. https://doi.org/10.1155/2016/9128050.
17. Wu, L., Zhao, F., Dai, M., Li, H., Chen, C., Nie, J., Wang, P., and Wang, D.W. (2017). P2y12 Receptor Promotes Pressure Overload-Induced Cardiac Remodeling via Platelet-Driven Inflammation in Mice. Hypertension *70*, 759–769. https://doi.org/10.1161/hypertensionaha.117.09262.
18. Antonino, M.J., Mahla, E., Bliden, K.P., Tantry, U.S., and Gurbel, P.A. (2009). Effect of long-term clopidogrel treatment on platelet function and inflammation in patients undergoing coronary arterial stenting. Am. J. Cardiol. *103*, 1546–1550. https://doi.org/10.1016/j.amjcard.2009.01.367.
19. Li, H.Q., Liu, N., Zheng, Z.Y., Teng, H.L., and Pei, J. (2022). Clopidogrel delays and can reverse diabetic nephropathy pathogenesis

in type 2 diabetic db/db mice. World J. Diabetes *13*, 600–612. https://doi.org/10.4239/wjd.v13.i8.600.

20. Zheng, Z., Ma, T., Lian, X., Gao, J., Wang, W., Weng, W., Lu, X., Sun, W., Cheng, Y., Fu, Y., et al. (2019). Clopidogrel Reduces Fibronectin Accumulation and Improves Diabetes-Induced Renal Fibrosis. Int. J. Biol. Sci. *15*, 239–252. https://doi.org/10.7150/ijbs.29063.
21. Ito, M., Nakano, M., Ariyama, H., Yamaguchi, K., Tanaka, R., Semba, Y., Sugio, T., Miyawaki, K., Kikushige, Y., Mizuno, S., et al. (2022). Macrophages are primed to transdifferentiate into fibroblasts in malignant ascites and pleural effusions. Cancer Lett. *532*, 215597. https://doi.org/10.1016/j.canlet.2022.215597.
22. Zeng, F., Gao, M., Liao, S., Zhou, Z., Luo, G., and Zhou, Y. (2023). Role and mechanism of CD90(+) fibroblasts in inflammatory diseases and malignant tumors. Mol. Med. *29*, 20. https://doi.org/10.1186/s10020-023-00616-7.
23. Dong, L., Li, J.C., Hu, Z.J., Huang, X.R., Wang, L., Wang, H.L., Ma, R.C.W., Lan, H.Y., and Yang, S.J. (2021). Deletion of Smad3 protects against diabetic myocardiopathy in db/db mice. J. Cell. Mol. Med. *25*, 4860–4869. https://doi.org/10.1111/jcmm.16464.
24. Weiskirchen, R., Weiskirchen, S., and Tacke, F. (2019). Organ and tissue fibrosis: Molecular signals, cellular mechanisms and translational implications. Mol. Aspects Med. *65*, 2–15. https://doi.org/10.1016/j.mam.2018.06.003.
25. Fang, Q., Wang, J., Wang, L., Zhang, Y., Yin, H., Li, Y., Tong, C., Liang, G., and Zheng, C. (2015). Attenuation of inflammatory response by a novel chalcone protects kidney and heart from hyperglycemia-induced injuries in type 1 diabetic mice. Toxicol. Appl. Pharmacol. *288*, 179–191. https://doi.org/10.1016/j.taap.2015.07.009.
26. Jiang, F., Liu, G.S., Dusting, G.J., and Chan, E.C. (2014). NADPH oxidase-dependent redox signaling in TGF-β-mediated fibrotic responses. Redox Biol. *2*, 267–272. https://doi.org/10.1016/j.redox.2014.01.012.
27. Yao, H., He, Q., Huang, C., Wei, S., Gong, Y., Li, X., Liu, W., Xu, Z., Wu, H., Zheng, C., and Gao, Y. (2022). Panaxatriol saponin ameliorates myocardial infarction-induced cardiac fibrosis by targeting Keap1/Nrf2 to regulate oxidative stress and inhibit cardiac-fibroblast activation and proliferation. Free Radic. Biol. Med. *190*, 264–275. https://doi.org/10.1016/j.freeradbiomed.2022.08.016.
28. An, X., Jiang, G., Cheng, C., Lv, Z., Liu, Y., and Wang, F. (2018). Inhibition of Platelets by Clopidogrel Suppressed Ang II-Induced Vascular Inflammation, Oxidative Stress, and Remodeling. J. Am. Heart Assoc. *7*, e009600. https://doi.org/10.1161/jaha.118.009600.
29. Gibb, A.A., Lazaropoulos, M.P., and Elrod, J.W. (2020). Myofibroblasts and Fibrosis: Mitochondrial and Metabolic Control of Cellular Differentiation. Circ. Res. *127*, 427–447. https://doi.org/10.1161/circresaha.120.316958.
30. Hartupee, J., and Mann, D.L. (2016). Role of inflammatory cells in fibroblast activation. J. Mol. Cell. Cardiol. *93*, 143–148. https://doi.org/10.1016/j.yjmcc.2015.11.016.
31. Kalluri, R., and Neilson, E.G. (2003). Epithelial-mesenchymal transition and its implications for fibrosis. J. Clin. Invest. *112*, 1776–1784. https://doi.org/10.1172/jci20530.
32. Zeisberg, E.M., Tarnavski, O., Zeisberg, M., Dorfman, A.L., McMullen, J.R., Gustafsson, E., Chandraker, A., Yuan, X., Pu, W.T., Roberts, A.B., et al. (2007). Endothelial-to-mesenchymal transition contributes to cardiac fibrosis. Nat. Med. *13*, 952–961. https://doi.org/10.1038/nm1613.
33. Wessels, A., and Pérez-Pomares, J.M. (2004). The epicardium and epicardially derived cells (EPDCs) as cardiac stem cells. Anat. Rec. A Discov. Mol. Cell. Evol. Biol. *276*, 43–57. https://doi.org/10.1002/ar.a.10129.
34. Meng, L., Lu, Y., Wang, X., Cheng, C., Xue, F., Xie, L., Zhang, Y., Sui, W., Zhang, M., Zhang, Y., and Zhang, C. (2023). NPRC deletion attenuates cardiac fibrosis in diabetic mice by activating PKA/PKG and inhibiting TGF-β1/Smad pathways. Sci. Adv. *9*, eadd4222. https://doi.org/10.1126/sciadv.add4222.
35. Chen, Z., Zheng, L., and Chen, G. (2023). 2-Arachidonoylglycerol Attenuates Myocardial Fibrosis in Diabetic Mice Via the TGF-β1/Smad Pathway. Cardiovasc. Drugs Ther. *37*, 647–654. https://doi.org/10.1007/s10557-021-07307-7.
36. Haider, N., Boscá, L., Zandbergen, H.R., Kovacic, J.C., Narula, N., González-Ramos, S., Fernandez-Velasco, M., Agrawal, S., Paz-García, M., Gupta, S., et al. (2019). Transition of Macrophages to Fibroblast-Like Cells in Healing Myocardial Infarction. J. Am. Coll. Cardiol. *74*, 3124–3135. https://doi.org/10.1016/j.jacc.2019.10.036.
37. Mouton, A.J., DeLeon-Pennell, K.Y., Rivera Gonzalez, O.J., Flynn, E.R., Freeman, T.C., Saucerman, J.J., Garrett, M.R., Ma, Y., Harmancey, R., and Lindsey, M.L. (2018). Mapping macrophage polarization over the myocardial infarction time continuum. Basic Res. Cardiol. *113*, 26. https://doi.org/10.1007/s00395-018-0686-x.
38. Hu, L., Chang, L., Zhang, Y., Zhai, L., Zhang, S., Qi, Z., Yan, H., Yan, Y., Luo, X., Zhang, S., et al. (2017). Platelets Express Activated P2Y(12) Receptor in Patients With Diabetes Mellitus. Circulation *136*, 817–833. https://doi.org/10.1161/circulationaha.116.026995.
39. Lurje, I., Gaisa, N.T., Weiskirchen, R., and Tacke, F. (2023). Mechanisms of organ fibrosis: Emerging concepts and implications for novel treatment strategies. Mol. Aspects Med. *92*, 101191. https://doi.org/10.1016/j.mam.2023.101191.
40. Geng, T., Zhu, K., Lu, Q., Wan, Z., Chen, X., Liu, L., Pan, A., and Liu, G. (2023). Healthy lifestyle behaviors, mediating biomarkers, and risk of microvascular complications among individuals with type 2 diabetes: A cohort study. PLoS Med. *20*, e1004135. https://doi.org/10.1371/journal.pmed.1004135.
41. Milionis, H., Ntaios, G., Papavasileiou, V., Spengos, K., Manios, E., Elisaf, M., and Vemmos, K. (2017). Aspirin Versus Clopidogrel for Type 2 Diabetic Patients with First-Ever Noncardioembolic Acute Ischemic Stroke: Ten-Year Survival Data from the Athens Stroke Outcome Project. J. Stroke Cerebrovasc. Dis. *26*, 2769–2777. https://doi.org/10.1016/j.jstrokecerebrovasdis.2017.06.052.
42. Kuang, S., He, F., Liu, G., Sun, X., Dai, J., Chi, A., Tang, Y., Li, Z., Gao, Y., Deng, C., et al. (2021). CCR2-engineered mesenchymal stromal cells accelerate diabetic wound healing by restoring immunological homeostasis. Biomaterials *275*, 120963. https://doi.org/10.1016/j.biomaterials.2021.120963.
43. Gong, M., Guo, Y., Dong, H., Wu, W., Wu, F., and Lu, F. (2023). Trigonelline inhibits tubular epithelial-mesenchymal transformation in diabetic kidney disease via targeting Smad7. Biomed. Pharmacother. *168*, 115747. https://doi.org/10.1016/j.biopha.2023.115747.
44. Zhang, Y., Han, S., Liu, C., Zheng, Y., Li, H., Gao, F., Bian, Y., Liu, X., Liu, H., Hu, S., et al. (2023). THADA inhibition in mice protects against type 2 diabetes mellitus by improving pancreatic β-cell function and preserving β-cell mass. Nat. Commun. *14*, 1020. https://doi.org/10.1038/s41467-023-36680-0.
45. Zhan, J., Jin, K., Ding, N., Zhou, Y., Hu, G., Yuan, S., Xie, R., Wen, Z., Chen, C., Li, H., and Wang, D.W. (2023). Positive feedback loop of miR-320 and CD36 regulates the hyperglycemic memory-induced diabetic diastolic cardiac dysfunction. Mol. Ther. Nucleic Acids *31*, 122–138. https://doi.org/10.1016/j.omtn.2022.12.009.
46. Wu, Q.R., Zheng, D.L., Liu, P.M., Yang, H., Li, L.A., Kuang, S.J., Lai, Y.Y., Rao, F., Xue, Y.M., Lin, J.J., et al. (2021). High glucose induces Drp1-mediated mitochondrial fission via the Orai1 calcium channel to participate in diabetic cardiomyocyte hypertrophy. Cell Death Dis. *12*, 216. https://doi.org/10.1038/s41419-021-03502-4.
47. Zhang, B., Li, X., Liu, G., Zhang, C., Zhang, X., Shen, Q., Sun, G., and Sun, X. (2021). Peroxiredomin-4 ameliorates lipotoxicity-induced oxidative stress and apoptosis in diabetic cardiomyopathy. Biomed. Pharmacother. *141*, 111780. https://doi.org/10.1016/j.biopha.2021.111780.
48. Hashimoto, M., Sugidachi, A., Isobe, T., Niitsu, Y., Ogawa, T., Jakubowski, J.A., and Asai, F. (2007). The influence of P2Y12 receptor deficiency on the platelet inhibitory activities of prasugrel in a mouse model: evidence for specific inhibition of P2Y12 receptors by prasugrel. Biochem. Pharmacol. *74*, 1003–1009. https://doi.org/10.1016/j.bcp.2007.06.027.
49. Wang, L.F., Li, Q., Wen, K., Zhao, Q.H., Zhang, Y.T., Zhao, J.L., Ding, Q., Guan, X.H., Xiao, Y.F., Deng, K.Y., and Xin, H.B. (2023). CD38 Deficiency Alleviates Diabetic Cardiomyopathy by Coordinately Inhibiting Pyroptosis and Apoptosis. Int. J. Mol. Sci. *24*, 16008. https://doi.org/10.3390/ijms242116008.
50. Zhang, X., Duan, Y., Zhang, X., Jiang, M., Man, W., Zhang, Y., Wu, D., Zhang, J., Song, X., Li, C., et al. (2023). Adipsin alleviates cardiac microvascular injury in diabetic cardiomyopathy through Csk-dependent signaling mechanism. BMC Med. *21*, 197. https://doi.org/10.1186/s12916-023-02887-7.

STAR★METHODS

KEY RESOURCES TABLE

REAGENT or RESOURCE	SOURCE	IDENTIFIER
Antibodies		
Antibodies are listed in Table S1	This paper	N/A
Chemicals, peptides, and recombinant proteins		
Clopidogrel	MedChemExpress, USA	Cat# HY-15283
DMEM, low-glucose (5.5 mM of D-glucose)	Procell, China	Cat# PM150220
D-glucose	Procell, China	Cat# PB180418
Palmitic acid	Kunchuang Biotechnology, China	Cat# KC002
Wheat germ agglutinin	Sigma-Aldrich, USA	Cat# L4895
Rhodamine-Phalloidin	Servicebio, China	Cat# G1249-100T
Protease and Phosphatase Inhibitor Cocktail	NCM Biotech, China	Cat# P002
RIPA buffer	Beyotime, China	Cat# P0013B
Enhanced BCA Protein Assay Kit	Beyotime, China	Cat# P0010
Critical commercial assays		
Mouse TNF-alpha ELISA Kit	Proteintech, China	Cat# KE10002
Mouse IL-1 beta ELISA Kit	Proteintech, China	Cat# KE10003
Mouse IL-6 ELISA Kit	Proteintech, China	Cat# KE10091
Mouse MCP-1 ELISA Kit	Proteintech, China	Cat# KE10006
CK Activity Assay Kit	Elabscience Biotechnology Co., Ltd, China	Cat# E-BC-K558-S
Mouse CK-MB ELISA Kit	Elabscience Biotechnology Co., Ltd, China	Cat# E-EL-M0355c
Mouse LDH ELISA Kit	Elabscience Biotechnology Co., Ltd, China	Cat# E-EL-M0419c
3-NT(3-Nitrotyrosine) ELISA Kit	Elabscience Biotechnology Co., Ltd, China	Cat# E-EL-0040c
Lipid Peroxidation MDA Assay Kit	Beyotime, China	Cat# S0131S
Catalase Assay Kit	Beyotime, China	Cat# S0051
GSH and GSSG Assay Kit	Beyotime, China	Cat# S0053
Total SD Assay Kit with WST-8	Beyotime, China	Cat# S0101S
Animal Total RNA Isolation Kit	Foregene, China	Cat# RE-03014
Reverse Transcription System Kit	Monad, China	Cat# REF05101
2×RealStar Fast SYBR qPCR Mix (Low ROX)	GenStar, China	Cat# A303
Cell Counting Kit-8	NCM Biotech, China	Cat# C6005
ROS Assay Kit (DCFH-DA probe)	Beyotime, China	Cat# S0033S
Experimental models: Cell lines		
AC16 cells	EK-Bioscience Biotechnology Co., Ltd, China	Cat# CC-Y1760; RRID: CVCL_4U18
Experimental models: Organisms/strains		
Mouse: C57BLKS db/db (C57BLKS-Lepr$^{-/-}$)	Gempharmatech Co., Ltd, China	Cat# T002407
Oligonucleotides		
Primers are listed in Table S2	This paper	N/A
Software and algorithms		
GraphPad Prism 8 software	GraphPad Software Inc., San Diego, CA, USA	N/A
ImageJ software	US National Institutes of Health, Bethesda, MD, USA	N/A

RESOURCE AVAILABILITY

Lead contact

Further information and requests for resources and reagents should be directed to and will be fulfilled by the lead contact, He Cai (caihe19@mails.jlu.edu.cn).

Materials availability

This study did not generate new unique reagents.

Data and code availability

- Data reported in this paper will be shared by the lead contact upon request.
- This paper does not report original code.
- Any additional information required to reanalyse the data reported in this paper is available from the lead contact upon request.

EXPERIMENTAL MODEL AND STUDY PARTICIPANT DETAILS

Mouse models

Four-week-old male db/m (C57BLKS/JGpt) and db/db (Strain NO. T002407, BKS-Leprem2Cd479/Gpt) mice were purchased from GemPharmatech Co., Ltd (Jiangsu, China). The db/db mouse line has been extensively employed as a model for as a model for investigating type 2 diabetes,[42–44] including for the studies on DCM of type 2 diabetes.[45–47] Mice were housed at the School of Translational Medicine, Jilin University, under standard conditions (22°C, 12-h/12-h light/dark cycle) with *ad libitum* access to food and water. All animal experiments were approved by the ethics committee of the First Hospital of Jilin University and conformed to the internationally accepted principles for the care and use of laboratory animals. The experimental procedure is presented in Figure S4. All mice were fed until 3 months of age without any treatment, and this time point was defined as the baseline. The mice were divided into six groups as follows: (1) db/m mice + vehicle (CON group), (2) db/m mice + middle-dose Clo (10 mg/kg/day) treatment (CON + Clo group), (3) db/db mice + vehicle (DM group), (4) db/db mice + low-dose Clo (5 mg/kg/day) treatment (DM + Clo ^{L} group), (5) db/db mice + middle-dose Clo (10 mg/kg/day) treatment (DM + Clo ^{M} group), and (6) db/db mice + high-dose Clo (20 mg/kg/day) treatment (DM + Clo ^{H} group). The mice were administered Clo or vehicle daily by gavage for 5 months. At the end of the experiment, the mice were intraperitoneally anaesthetized with pentobarbital and sacrificed to collect blood and cardiac ventricular tissues for subsequent experiments. Starting at the cardiac apex and parallel to the base of the heart, approximately 20 mg of apical tissue was collected for mRNA analysis, after which approximately 3 mm thick circular heart tissue was collected for histological analysis. The remaining cardiac ventricular tissues were subjected to Western blot analysis. Clo, sourced from MedChemExpress (HY-15283, Monmouth Junction, NJ, USA), was administered at varying doses (5/10/20 mg/kg/day) based on previous studies.[20,28,48] Those studies demonstrated that 5 mg/kg/day Clo effectively suppressed angiotensin II-induced vascular remodelling in mice, while 20 mg/kg/day Clo improved diabetes-induced renal fibrosis. Consequently, our study employed these escalating doses (5/10/20 mg/kg/day) of Clo to explore their effects on DCM. All experiments involving mice were conducted in accordance with the ethical guidelines of the Animal Ethics Committee of First Hospital of Jilin University.

Cell lines and cell culture

The AC16 human cardiomyocyte cell line was obtained from EK-Bioscience Biotechnology Co., Ltd. (CC-Y1760, Shanghai, China) and validated by the STR profiling method. The cells were cultured in low-glucose (5.5 mM D-glucose) Dulbecco's modified Eagle's medium (DMEM; PM150220, Procell, Wuhan, China) supplemented with 10% foetal bovine serum (164210-50, Procell) and 1% penicillin/streptomycin (PB180120, Procell) in a humidified incubator with 5% CO2 at 37°C. The glucolipotoxicity-induced injury of cardiomyocytes by PA + HG has been widely used for *in vitro* studies of diabetic cardiomyopathy.[49,50] Thus, the AC16 cells were treated as follows: (1) NC group: 5 mM glucose and solvent control of PA; (2) PA + HG group: 300 μM PA (KC002, Kunchuang Biotechnology, Xian, China) and 33 mM HG (PB180418, Procell); (3) PA + HG + Clo group: 300 μM PA, 33 mM HG, and 10 μM Clo. In the present study, AC16 cells were pretreated with 10 μM Clo for 1 h and subsequently exposed to 33 mM HG + 300 μM PA for 48 h.

METHOD DETAILS

Echocardiography

Cardiac function was assessed via transthoracic echocardiography. Briefly, mice were anesthetized with pentobarbital after their chest hair was shaved, and the mice were laid flat on their backs on a plate. Left ventricular EF, left ventricular FS, LVPWd, LVIDd, and the MV E/A ratio were measured via echocardiography.

Blood glucose levels and blood clotting times

Blood glucose levels (3-h fasting blood glucose) and blood clotting time were measured through the tail vein of the mice. Blood clotting time was measured by a mouse tail vein bleeding assay.[20] Briefly, the mice were anesthetized with pentobarbital, and their tails were cleaned with a

sterile cotton ball. Next, the tail of each mouse was cut 1–2 mm from the tip and immediately immersed in saline (at 37°C), after which the bleeding time was recorded.

Measurement of serum lipid levels in mice

Total cholesterol (A111-1-1, Nanjing Jiancheng, Jiangsu, China) and triglyceride (A110-1-1, Nanjing Jiancheng) levels in the serum samples were measured via commercial kits following the manufacturer's protocols.

Measurement of inflammatory marker levels in serum

To assess the inflammatory response in mice, mouse ELISA kits were used to measure the serum levels of TNF-α (KE10002, Proteintech), IL-1β (KE10003, Proteintech), IL-6 (KE10091, Proteintech), and MCP-1 (KE10006, Proteintech) according to the manufacturer's protocol.

Evaluation of cardiac marker levels in serum

The serum levels of cardiac biomarkers, including CK (E-BC-K558-S, Elabscience Biotechnology Co., Ltd., Wuhan, China), CK-MB (E-EL-M0355c, Elabscience Biotechnology Co., Ltd.), and LDH (E-EL-M0419c, Elabscience Biotechnology Co., Ltd.), were measured in mice using commercial kits and according to the manufacturer's protocol.

Assessment of oxidative stress

SOD and CAT are the dominant antioxidant enzymes in the body, and they eliminate oxygen radicals to reduce oxidative damage. GSH is a nonenzymatic antioxidant, and its content reflects the antioxidant capacity of the body to a certain extent. As oxidative stress can lead to lipid peroxidation, the levels of the lipid peroxidation product MDA can reflect the extent of lipid peroxidation. To assess oxidative stress levels in mouse heart tissue, GSH (S0053, Beyotime, Shanghai, China), SOD (S0101S, Beyotime), CAT (S0051, Beyotime), MDA (S0131S, Beyotime), and 3-NT (E-EL-0040c, Elabscience Biotechnology Co., Ltd.) levels were measured using commercial kits according to the manufacturers' instructions.

Histology

The collected cardiac ventricular tissues were fixed with 4% paraformaldehyde and embedded in paraffin. Hematoxylin and eosin (H&E), Masson (G1006, Servicebio, Wuhan, China), immunohistochemistry, immunofluorescence, and WGA staining were performed on paraffin-embedded sections. Images of the stained sections were captured through observation under an inverted light microscope or fluorescence microscope (IX73, Olympus, Japan). Six different fields per section were randomly chosen for analysis using ImageJ software (US National Institutes of Health, Bethesda, MD, USA).

Immunohistochemistry

For immunohistochemical staining, after antigen repair, endogenous peroxidase blocking with 3% hydrogen peroxide solution, and serum closure with 3% BSA, the slides were incubated with primary antibodies against COL1A1 (1:500, ab138492, Abcam, Cambridge, UK), TGF-β1 (1:500, ab215715, Abcam), and Fibronectin (1:500, ab2413, Abcam) overnight at 4°C. Next, the slides were incubated with secondary antibodies conjugated to horseradish peroxidase (HRP) for 1 h and DAB colour developing solution for detection.

Immunofluorescence

For immunofluorescence staining, following heat-induced antigen repair and blocking with 3% BSA, the slides were incubated with F4/80 (29414-1-AP, Proteintech), α-SMA (14395-1-AP, Proteintech), or CD90 (P01831, Servicebio) primary antibody overnight at 4°C, followed by incubation for 1 h at room temperature with the secondary antibody and staining with DAPI for 10 min.

WGA staining

For WGA staining, after heat-induced antigen repair with EDTA antigen repair buffer, the slides were incubated with FITC-conjugated WGA (L4895, Sigma–Aldrich, St. Louis, MO, USA) for 1 h at 37°C, followed by staining with DAPI for 10 min.

Nuclear protein extraction

Nuclear protein was extracted using a Nuclear Protein Extraction Kit (P0027, Beyotime) according to the manufacturer's protocol.

Western blotting

Protein was extracted from cardiac ventricular tissue or AC16 cells in RIPA buffer (P0013B, Beyotime), which included protease and phosphatase inhibitors (P002, NCM Biotech). The protein concentration was determined using a BCA assay kit (P0010, Beyotime). Subsequently, 30 μg of total protein was separated on SDS–PAGE gels at 80–120 V and transferred onto PVDF membranes (IPVH00010, Merck KGaA, Darmstadt, Germany) with a 0.45-μm pore size at 100 V for 1–2 h based on the molecular weight of the target protein. The membranes were blocked in 5% nonfat milk for 2 h at room temperature, followed by an overnight incubation with the primary antibody at 4°C. Subsequently, the membranes

were incubated with the corresponding HRP-conjugated secondary antibodies for 1 h at room temperature, after which the proteins were detected using an enhanced chemiluminescence (ECL) detection kit (Bio-Rad, Hercules, CA, USA). The original grey levels determined by Western blotting were analysed using ImageJ software, and the ratio of the grayscale value of the target protein to the grayscale value of the reference protein was calculated. This ratio serves as a quantitative representation of the relative expression levels. The antibody dilution information is provided in Table S1.

Real-time qPCR

Total RNA was extracted from heart tissue or cells using an Animal Total RNA Isolation Kit (RE-03014, Foregene, Chengdu, China) or a Cell Total RNA Isolation Kit (RE-03111, Foregene). Total RNA was reverse transcribed into cDNA using a Reverse Transcription System Kit (REF05101, Monad, Wuhan, China). Real-time qPCR was performed using SYBR Green (A303, GenStar, Tianjin, China). The expression of the target genes was normalized to that of the reference gene GAPDH and quantified using the $2^{-\Delta\Delta CT}$ method. The primer sequences are listed in Table S2.

Cell viability assay

Cell proliferation was assessed using a CCK-8 (C6005, NCM Biotech, Suzhou, China) according to the manufacturer's instructions. Briefly, 100 μL of cell suspension containing 6,000 cells was seeded in 96-well plates and treated with PA + HG or Clo at increasing concentrations for 48 h. Then, the cell culture medium was changed, and 10 μL of CCK-8 solution was added to each well, followed by incubation at 37°C in a 5% CO2 atmosphere for 1–2 h. Absorbance at 450 nm was measured to determine cell viability.

Rhodamine-phalloidin staining

AC16 cells were fixed with 4% paraformaldehyde at room temperature for 30 min and then permeabilized with 0.3% Triton X-100 for 10 min, followed by staining with rhodamine-phalloidin (G1249-100T, Servicebio) at a final concentration of 100 nM for 30 min. DAPI was used to stain the nucleus. Images were acquired by observation under an inverted fluorescence microscope (IX73, Olympus, Japan) and analysed using ImageJ software.

ROS levels in the cells

Intracellular ROS contents were measured via DCFH-DA fluorescence staining (S0033S, Beyotime) according to the manufacturer's protocol. Fluorescence images were collected using an inverted fluorescence microscope (IX73, Olympus, Japan) and analysed using ImageJ software.

QUANTIFICATION AND STATISTICAL ANALYSIS

Data are presented as the mean ± SEM. Multiple comparisons were performed using one-way analysis of variance (one-way ANOVA), followed by Tukey's test for pairwise multiple comparisons. All the statistical tests were two-tailed, and $P < 0.05$ was considered indicative of statistical significance. GraphPad Prism 8 (GraphPad Software Inc., San Diego, CA, USA) was used to perform the data analysis and graphing.